Quaternary Research 75 (2011) 1–10

Contents lists available at ScienceDirect

Quaternary Research

journal homepage: www.elsevier.com/locate/yqres

Late Quaternary glacial chronology on Nevado Illimani, Bolivia, and the implications for paleoclimatic reconstructions across the Andes

Colby A. Smith [a,*], Thomas V. Lowell [a], Lewis A. Owen [a], Marc W. Caffee [b]

[a] Department of Geology, University of Cincinnati, Cincinnati, OH, USA
[b] PRIME Lab, Purdue University, West Lafayette, IN, USA

ARTICLE INFO

Article history:
Received 27 April 2009
Available online 21 August 2010

Keywords:
Glacial geology
Tropical Andes
Glacial chronology
Bolivia
Nevado Illimani
Cordillera Real
Equilibrium line altitude

ABSTRACT

^{10}Be terrestrial cosmogenic nuclide surface exposure ages from moraines on Nevado Illimani, Cordillera Real, Bolivia suggest that glaciers retreated from moraines during the periods 15.5–13.0 ka, 10.0–8.5 ka, and 3.5–2.0 ka. Late glacial moraines at Illimani are associated with an ELA depression of 400–600 m, which is consistent with other local reconstructions of late glacial ELAs in the Eastern Cordillera of the central Andes. A comparison of late glacial ELAs between the Eastern Cordillera and Western Cordillera indicates a marked change toward flattening of the east-to-west regional ELA gradient. This flattening is consistent with increased precipitation from the Pacific during the late glacial period.

Introduction

Paleoclimate records from the Altiplano and central Andes are ambiguous regarding the chronology of moisture sources during the late glacial period. Lake-level data from Lake Titicaca have been used to suggest both a wet period between 13.0 and 11.5 ka (Baker et al., 2001a) and a dry period between ~14.5 and 11.5 ka (Rowe et al., 2003). Farther south on the Altiplano, paleo-shorelines (Placzek et al., 2006) and lacustrine deposits (Baker et al., 2001b) of what is now the Salar de Uyuni suggest wet conditions in the late glacial between 13.0 and 11.0 ka and after 12.5 ka, respectively. At higher elevations, oxygen isotopic data from tropical Andean ice cores (Thompson et al., 1995, 1998; Ramirez et al., 2003) show a marked decrease in isotopic values between ~14.0 and 11.5 ka (Thompson et al., 1998). This change in isotopic values has been interpreted to indicate either cooler (Thompson et al., 1995) or wetter (Ramirez et al., 2003) conditions. Although the exact chronology of aridity during the late glacial remains to be worked out, the pattern shown in isotopic records from the ice cores appears to be correct. Following the wet glacial period there was a relative dry period, followed by a relative wet period (termed the deglacial climatic reversal by Thompson et al., 1998), followed by the early Holocene arid period with generally increasing humidity through the Holocene.

Additionally, the source of the hypothesized increase in precipitation during the late glacial is debated. Haug et al. (2001) and Baker et al. (2001b) suggest that the increased precipitation may have been advected to the Altiplano from the Atlantic as a result of the southward displacement of the intertropical convergence zone and the strengthening of the South American summer monsoon. Alternatively, Heusser (1981), based on pollen analysis, suggests the increased precipitation may have originated in the Pacific and been transported to the Altiplano by winter storms associated with the northward displacement of the westerly wind system. This view is supported in part by more recent work in the Atacama desert. Maldonado et al. (2005) suggest that the period between 24 and 11 ka was wetter than today based on dated pollen assemblages in rodent middens. Moreover, based on the different pollen records found at different elevations Maldonado et al. (2005) suggest that the increased precipitation was derived from different sources. From 24 to 17 ka the moisture came from the west; from 17 to 14 ka it came from both the east and west; and from 14 to 11 ka it came from the east.

The glacial geologic record can help reconstruct the timing of paleoclimate change, including regional precipitation gradients. In particular, reconstructed former glacial ELAs can be used to derive paleoclimatic conditions, which are a combination of temperature and precipitation. The regional ELA gradient reflects the regional precipitation gradient and can be used to extract the precipitation source (Harrison, 2005; Benn et al., 2005). For example, modern glacial ELAs and extents in the Eastern Cordillera are hundreds of meters lower than glaciers in the Western Cordillera (Francou et al., 1995; Klein et al., 1999; Jordan, 1999) despite having essentially the same temperatures at both locations. The rise in ELA to the west is a result of decreasing precipitation to the west. Examining the ELAs in both the Eastern and Western Cordilleras over time can provide hints as to the

* Corresponding author.
E-mail address: casmith@stlawu.edu (C.A. Smith).

0033-5894/$ – see front matter
doi:10.1016/j.yqres.2010.07.001

regional precipitation gradient and the source of the precipitation. For example, reconnaissance work on undated moraines by Hastenrath (1971) suggests that ELA depression was greater to the south and west during the “Pleistocene”. These results led Hastenrath (1971) to hypothesize a western source of moisture.

Existing paleo-ELA records are derived largely from the Eastern Cordillera. For the late glacial, Seltzer (1992, 1994) calculates ΔELAs of 300–500 m in the Cordillera Real; Mark et al. (2002) estimated ΔELAs of 170–230 m in the Cordillera Vilcanota and at the Quelccaya Ice-cap. For the period about 32 ka, Smith et al. (2005) reported ΔELAs of 300–600 m on the Junin Plain and the west side of the Cordillera Real. Smith et al. (2005) reported a ΔELA of 800–1000 m in one location on the east side of the Cordillera Real. Although Smith et al. (2005) mapped and dated late glacial moraines, ΔELAs are provided only from moraines that date to ~32 ka. Therefore, the late glacial moraines that are inset to the 32 ka moraines would have smaller ΔELAs.

The purpose of this study is to combine ^{10}Be cosmogenic nuclide surface exposure dating with geomorphic mapping to reconstruct a chronology of late glacial and Holocene glacial extents near Nevado Illimani, Eastern Cordillera, Bolivia. This record of glaciation is then compared with other existing paleoclimate chronologies of the tropical Andes to help resolve issues concerning changes in temperature and precipitation during the late Quaternary and early Holocene. Finally, reconstructed elevations of late glacial ELAs are used to make inferences about principal moisture sources and changes in tropical atmospheric circulation during the late glacial.

Geologic setting

Fieldwork for the present study was conducted in Pasto Grande Valley between 4000 m and 5200 m above sea level (asl) on the north side of Nevado Illimani in the Cordillera Real, Bolivia (Fig. 1). The Cordillera Real is a range of 6000-m-high peaks in the Eastern Cordillera that bounds the east side of the Altiplano, a high-elevation plateau at about 3800 masl. Currently, precipitation in the region originates from the tropical Atlantic and is transported seasonally over the continent during the South American Summer Monsoon (Zhou and Lau, 1998). While some cities in the Beni region east of the Eastern Cordillera receive over 2000 mm of rain per year (SENAHAMI website), the Altiplano is semi-arid. The intensively studied Zongo Glacier, about 60 km northwest of Illimani along the axis of the Cordillera Real, provides a good source of meteorological data. There the mean annual precipitation for hydrological years 1992–1996 was 794 mm, and the mean annual temperature was 7.2°C at 3922 masl (Francou et al., 1995; Wagnon, et al., 1999). The mean annual 0°C isotherm is at about 4895 masl using a lapse rate of 7.4°C/km (Francou et al., 1995), in conjunction with the measured temperature at 3922 masl. Modern glaciers in Pasto Grande Valley extend to about 4900 masl apparently terminating at the mean annual 0°C isotherm.

Methods

Geomorphic mapping of the field area allowed for a better understanding of the morphostratigraphic relationships between glacial geomorphic landforms. The map, constructed from Bolivian aerial photograph number 1052 taken in 1963, also serves to plot the twenty-three samples of granodiorite collected from moraines and dated using ^{10}Be exposure age methods (Gosse and Phillips, 2001).

When selecting rocks to sample, care was taken to choose large intact boulders that were unlikely to have been transported downslope or exhumed subsequent to deposition of the moraine. A minimum of 600 g was collected from nearly horizontal surfaces using

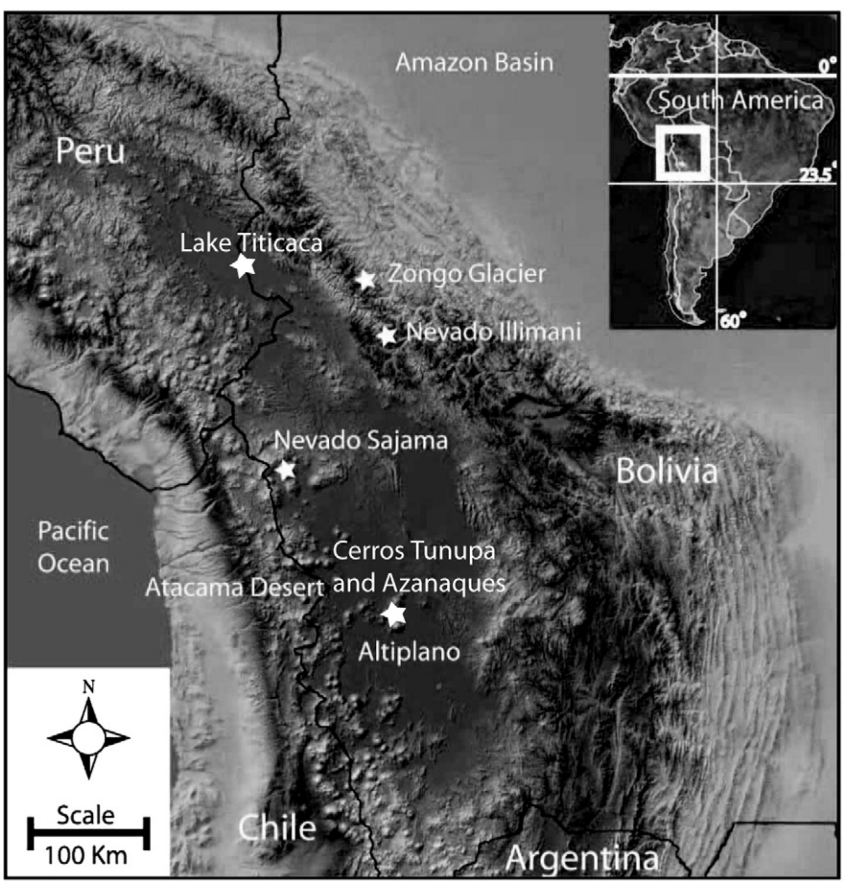

Figure 1. Digital elevation model of the Altiplano, showing the locations of key sites mentioned in the text. The box on the inset map of South America approximates the enlarged area of the DEM.

a hammer and chisel. Latitude, longitude, and elevation data were collected for each sample site using a handheld GPS. Topographic shielding values were measured with a pocket transit at 30° intervals.

Processing of the rock samples to isolate Be was carried out at the University of Cincinnati. Samples were crushed and sieved to isolate the 250–500 μm fraction. The samples were then leached in aqua regia overnight prior to two 24-h leachings in 5% HF/HNO_3. This was followed by heavy liquid (lithium heteropolytungstate) separation. Then the samples were leached a final time in 1% HF/HNO_3 for 24 h to obtain pure quartz.

Approximately 20 g of pure quartz from each sample were mixed with 1.26 mg/g Be carrier and dissolved in concentrated HF. Following perchloric acid fuming, the samples were passed through anion and cation exchange columns. The Be fraction was collected and precipitated with ammonium hydroxide. The resultant beryllium hydroxide gel was rinsed before being oxidized in quartz crucibles at 750°C for 5 min to produce beryllium oxide. Nb powder was mixed with beryllium oxide and the combination was pounded into stainless steel targets for measurement of $^{10}Be/^{9}Be$ ratios by accelerator mass spectrometry at PRIME Laboratory, Purdue University.

SPEX beryllium standard (Trace ICP/ICP-MS grade) at 1000 μg/ml in 2% HNO_3 was used for all samples and blanks. Three blanks were processed and chemical data are presented in Table 1. All reported ^{10}Be ages were calculated using the CRONUS Laboratory Age Calculator with a production rate of 4.5 ^{10}Be atoms/yr and a half-life of 1.36 Ma (Balco et al., 2008). The PRIME Laboratory accelerator mass spectrometry was calibrated using standard 200500020 from KN Standard Be 0152 with a ^{10}Be/total Be ratio of $9465\times°10^{-15}$.

We understand that there are a number of different scaling schemes and that, depending on which one is used, ages may vary by upwards of 20%. Changing the age of deposits by this magnitude may alter some of the climatic interpretations. Should the reader wish, the data needed to re-calculate ages using different scaling values are present in Table 2. Ages calculated using a number of different scaling schemes are present in Table 3. Given the uncertainty in scaling methods and the lack of a single standardized methodology, we use the scaling of Lal (1991) and Stone (2000) (Table 3) in the discussion of our data in order to allow for easy comparison to previously published exposure age data sets.

Results

Geomorphology of Pasto Grande Valley

Currently, three small separate glaciers feed into Pasto Grande Valley. Although the aerial photograph used as the base for the map (Fig. 2) had enough snow cover to make the two glaciers in the southwest tributary valley appear to be joined, they are in fact separate glaciers. These two glaciers would have been joined during deposition of even the youngest moraines. The youngest group of moraines, Group C, (Fig. 3) is composed of well-developed left and right lateral moraines that join terminal moraines and enclose a small pond at an elevation of 4785 masl. In this text, right and left lateral moraines refer to the positions of laterals when facing downvalley in the direction of ice flow. Hummocky debris, the upper portions of which are likely ice-cored, is inset to the Group C lateral moraines. A series of relic ice-contact fans grade to the Group C end moraines.

Table 1
Chemical data of blanks used for AMS measurement.

Blank name	Be carrier (g)	Carrier concentration (mg/g)	^{10}Be/total Be ratio	^{10}Be/total Be error
Cblk3	0.4091	1.26	1.795E-14	7.093E-15
Cblk4	0.3772	1.26	2.251E-14	5.497E-15
Cblk5	0.4022	1.26	1.398E-14	4.046E-15

About midway downvalley at an elevation of 4380 masl, two end moraines, cut by a small stream, perch atop a 120-m-high bedrock step in the valley floor. These end moraines, termed Group B, can be traced up into laterals that have been mostly removed by slope processes. Downvalley from the Group B end moraines, the valley drops steeply over the bedrock step. There are some traces of end moraines below the bedrock step, but they are poorly preserved due to stream incision. The associated lateral moraines are nearly buried in active scree.

A left lateral moraine terminates between Groups B and C at the junction with a southwest tributary valley. This moraine, part of Group A2, is much higher than the Group C moraines and represents an older, more extensive glacier configuration when all three glaciers coalesced. The single Group A2 left lateral can be traced downvalley where it becomes a series of smaller lateral moraines on the slope above the Group B end moraines before projecting over the bedrock step. The valley floor levels out downvalley from the bedrock step. Small fragments, <10 m in length, of both left and right lateral moraines of Group A remain along the valley walls. The lateral moraines are neither continuous nor well-preserved due to steep bedrock walls and active scree. Two end moraines, Group A1, cross the valley floor at an elevation of 4000 masl. The Group A1 end moraines are located just upvalley from a bedrock gorge. They are the outermost moraines dated in Pasto Grande Valley. Older fragments of lateral moraines extend out of Pasto Grande Valley and into Khañuma Valley, but these moraines were not dated as part of this study. These older moraines may date to the last glacial maximum, but in the absence of absolute ages all that is known for certain is that they predate the late glacial Group A moraines.

The lateral and end moraines of Group A are subdivided because the lateral moraines cannot be traced continuously to the end moraines. The longitudinal profiles for the left lateral moraine and the floor of the valley indicate that elevations of the lateral moraines project in a straight line to the terminal moraines. However, this would not be expected with the pronounced bedrock step. Rather, the laterals should more closely mimic the topography of the valley floor. Although either scenario is possible, the dearth of data points immediately below the bedrock step prevents a reliable correlation between the Groups A1 and A2 moraines. Thus, for the purpose of dating, Groups A1 and A2 are treated separately in our study.

ELA reconstructions

To reconstruct ELAs based on past glacial margins, we use the terminus-to-headwall altitude ratio (THAR) described by Meierding (1982) and Porter (2001), with a THAR value of 0.37 as suggested by Seltzer (1992) while working in the Cordillera Real. Also, we use the summit elevation (6350 masl) as that of the "headwall" because the glaciers extend to the summit of the mountain. Thus, former ELAs are calculated according to (Table 4):

$$ELA = (elevation\,of\,end\,moraine) + [0.37\,(6350\text{m} - elevation\,of\,end\,moraine)]$$

Changes in ELA are calculated by subtracting the estimates of the former ELA from 5270 masl, which is the mean ELA of Zongo Glacier for hydrological years 1992–1997 (Francou et al., 1995; Wagnon, et al., 1999).

As an alternative method, we also calculated the late glacial ELA using the accumulation-area ratio (AAR) method (Meierding, 1982; Porter, 2001; Benn et al., 2005). The late glacial extent and height of Pasto Grande Glacier were determined based on the positions of the dated Group A moraines on the 1:50,000, Cordillera Real Süd, topographic map published by the German Alpine Club (1990). The hypsometric data were derived from the map in 200 vertical meter segments.

Table 2
Locations, chemical data, and ^{10}Be surface exposure ages. Internal uncertainty refers to uncertainty associated with the AMS measurement.

Sample	Moraine group	Latitude	Longitude	Elev. (m)	Thickness (cm)	^{10}Be atoms/g	Error atoms/g	Shielding factor	Exposure age (ka)	Internal uncertainty (ka)
BV68	A1	16°34.60′S	67°47.77′W	4052	0.5	5.15E+05	1.28E-14	0.93	12.5	0.5
BV70	A1	16°34.56′S	67°47.69′W	4017	4.0	5.23E+05	1.37E-14	0.97	12.7	0.5
BV71	A1	16°34.56′S	67°47.69′W	3999	2.5	5.31E+05	1.72E-14	0.92	13.6	0.8
BV72	A1	16°34.55′S	67°47.66′W	3991	5.0	5.48E+05	2.52E-14	0.97	13.6	0.9
BV73	A1	16°34.53′S	67°47.67′W	3994	3.0	6.18E+05	5.85E-14	0.96	15.3	2.4
BV74	A1	16°34.53′S	67°47.67′W	3998	2.5	4.51E+05	1.89E-14	0.91	11.6	0.8
BV75	A1	16°34.52′S	67°47.67′W	4001	1.5	5.47E+05	1.38E-14	0.97	13.1	0.6
BV76	A1	16°34.52′S	67°47.64′W	3989	0.5	4.40E+05	1.53E-14	0.97	10.5	0.6
BV44	A2	16°36°11′S	67°47.80′W	4524	1.5	4.36E+05	1.50E-14	0.97	8.2	0.5
BV45	A2	16°36.14′S	67°47.82′W	4525	1.5	4.66E+05	1.83E-14	0.97	8.8	0.6
BV50	A2	16 35.22′S	67°47.78′W	4203	2.5	4.42E+05	1.44E-14	0.90	10.5	0.6
BV55	A2	16°35.92′S	67°47.74′W	4472	4.0	5.74E+05	2.16E-14	0.95	11.6	0.6
BV56	A2	16°35.92′S	67°47.73′W	4468	3.0	4.40E+05	1.49E-14	0.96	8.7	0.4
BV58	A2	16°35.92′S	67°47.73′W	4483	3.5	6.24E+05	4.40E-14	0.96	12.4	1.3
BV37	B	16°35.97′S	67°47.66′W	4405	4.0	4.20E+05	1.55E-14	0.95	8.7	0.5
BV38	B	16°35.98′S	67°47.67′W	4405	1.5	4.46E+05	1.69E-14	0.93	9.2	0.6
BV39	B	16°35.99′S	67°47.68′W	4427	2.0	4.09E+05	8.04E-15	0.95	8.2	0.3
BV52	B	16°35.89′S	67°47.60′W	4375	1.0	6.28E+05	3.41E-14	0.90	13.5	1.2
BV47	C	16°36.76′S	67°48.21′W	4880	2.5	1.22E+05	1.68E-14	0.92	2.1	0.5
BV49	C	16°36.75′S	67°48.18′W	4853	1.5	9.79E+04	1.09E-14	0.94	1.6	0.3
BV60	C	16°36.75′S	67°48.21′W	4816	2.5	1.19E+05	1.64E-14	0.87	2.2	0.5
BV61	C	16°36.75′S	67°48.22′W	4865	3.0	1.41E+05	2.58E-14	0.90	2.5	0.7

Seltzer (1992) suggested an AAR of 77% for the Cordillera Real. Use of this value in Pasto Grande Valley produces a late glacial ELA below the uppermost extent of the late glacial lateral moraine. Therefore, a lower AAR is required to produce a higher former ELA. Using an AAR of 66% yields a late glacial ELA of 4865 masl, which is only 5 m lower than that predicted by the THAR method. An AAR of 66% closely approximates the AAR of temperate latitude glaciers (Meierding, 1982) but is on the low side for tropical glaciers (Kaser and Osmaston, 2002; Benn et al., 2005). Based on the results of multiple methods, we estimate the late glacial ELA to be between 4680 and 4870 masl, which is between the maximum height of the lateral moraine (4680 masl) and the ELA calculation based on a THAR of 0.37 (4870 masl). These values indicate a lowering of the ELA by 400—590 m from modern values during the late glacial. Variables and values for ELA calculations are shown in Table 3.

Reconstructions of former ELAs using the THAR method are slightly higher than the maximum elevation of lateral moraines of the same ages for Groups C and A (assuming that A1 correlates with A2). In both cases the lateral moraines extend to steep bedrock faces where preservation is unlikely.

Ages of moraine groups

The ^{10}Be ages are presented as probability plots for each moraine group (Fig. 4) and as an age distance plot (Fig. 5). At a distance of several kilometers from the cirque headwall, exhumation is a far more common source of error than inheritance (Briner et al., 2005). While Briner et al. (2005) worked with deposits of cold-based glaciers, the predominance of exhumation-related errors is likely exacerbated when working with highly erosive wet-based glaciers that tend to

Table 3
Surface exposure ages calculated with different scaling methods.

		Lal (1991) and Stone (2000) time varying production rate		Desilets and Zreda (2003); Desilets et al. (2006)		Dunai (2001)		Lifton et al. (2005)		Lal (1991) and Stone (2000), constant production rate	
Sample	Moraine Group	Exposure age (ka)	External uncertainty	Exposure age (ka)	External uncertainty	Exposure age (ka)	External uncertainty	Exposure age (ka)	External uncertainty	Exposure age (ka)	External uncertainty
BV68	A1	12.5	1.2	10.4	1.3	10.5	1.3	10.4	1.1	12.1	1.2
BV70	A1	12.7	1.3	10.7	1.4	10.8	1.4	10.7	1.2	12.4	1.2
BV71	A1	13.6	1.5	11.4	1.6	11.5	1.6	11.4	1.4	13.2	1.4
BV72	A1	13.6	1.5	11.5	1.6	11.6	1.6	11.5	1.4	13.2	1.5
BV73	A1	15.3	2.8	12.9	2.6	13.1	2.6	12.9	2.5	14.8	2.7
BV74	A1	11.6	1.3	9.7	1.4	9.8	1.4	9.8	1.2	11.3	1.2
BV75	A1	13.1	1.3	11.0	1.4	11.1	1.4	11.0	1.2	12.8	1.3
BV76	A1	10.5	1.1	8.7	1.2	8.8	1.2	8.7	1.0	10.2	1.1
BV44	A2	8.2	0.9	6.6	0.9	6.6	0.9	6.6	0.8	7.8	0.8
BV45	A2	8.8	1.0	6.9	1.0	7.0	1.0	7.0	0.9	8.4	0.9
BV50	A2	10.5	1.1	8.5	1.2	8.6	1.2	8.5	1.0	10.2	1.1
BV55	A2	11.6	1.2	9.3	1.3	9.3	1.3	9.3	1.1	11.2	1.2
BV56	A2	8.7	0.9	7.1	0.9	7.3	1.0	7.1	0.8	8.0	0.8
BV58	A2	12.4	1.7	10.0	1.6	10.0	1.6	9.9	1.5	12.0	1.7
BV37	B	8.7	0.9	6.9	0.9	7.0	0.9	7.0	0.8	8.3	0.9
BV38	B	9.2	1.0	7.3	1.0	7.3	1.0	7.3	0.9	8.8	1.0
BV39	B	8.2	0.8	6.6	0.8	6.7	0.8	6.7	0.7	7.9	0.7
BV52	B	13.5	1.7	11.3	1.7	11.6	1.7	11.3	1.5	12.7	1.6
BV47	C	2.1	0.5	1.8	0.5	1.7	0.4	1.9	0.5	2.3	0.6
BV49	C	1.6	0.3	1.4	0.3	1.3	0.3	1.4	0.3	1.8	0.3
BV60	C	2.2	0.6	2.0	0.5	1.8	0.5	2.0	0.5	2.5	0.6
BV61	C	2.5	0.8	2.2	0.7	2.1	0.7	2.3	0.7	2.8	0.9

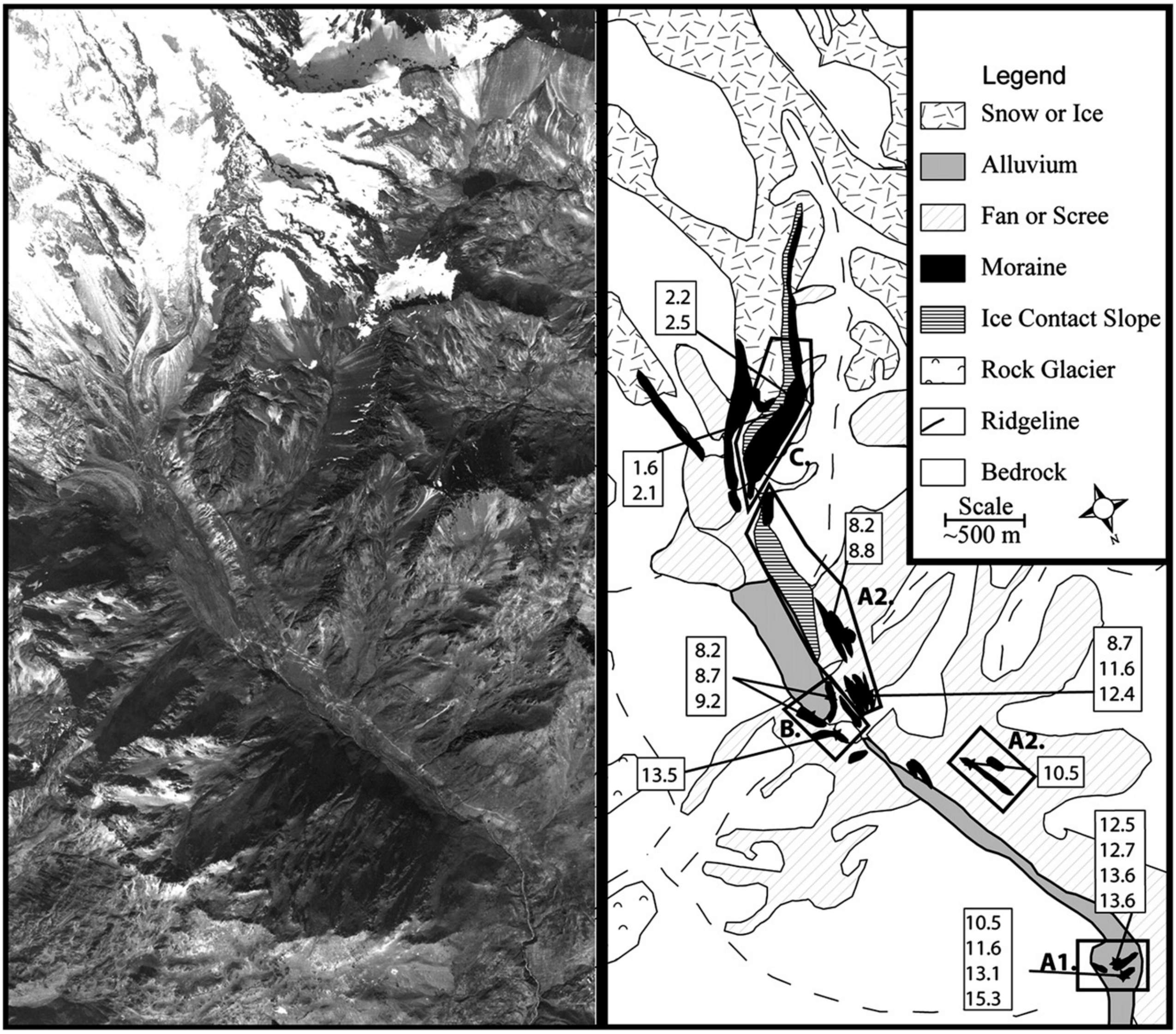

Figure 2. Aerial photograph and geomorphic map of Pasto Grande Valley on the north side of Nevado Illimani in the Cordillera Real. The moraines are sorted into four boxed Groups A1, A2, B, and C. The locations of samples are indicated by their assigned ages (ka).

limit inheritance. This has led some workers (Zreda et al., 1994; Phillips et al., 1997; Briner et al., 2005) to assign ages based on the single oldest date. While we do not select the oldest single sample we recognize that the age of a landform is likely to be on the older side of the distribution. Thus, we present minimum ages for stabilization of the moraines following the retreat of ice from the landforms.

Despite scaling-factor uncertainties, some firm conclusions can be reached. First, there were both early and late Holocene glacial expansions. Second, a late glacial stillstand or advance occurred.

Age-range assignments of the four groups of moraines are interpreted to fall between the peak of the probability distribution and the older end of the distribution (Fig. 4). Although the Group C moraines are not believed to be the result of a single advance insofar as the lateral moraine stratigraphy is complex, the final retreat from or stabilization of these compound moraines occurred after 3.5 ka and probably by 2.0 ka. Ice retreated from Group B moraines between 10.0 ka and 8.5 ka. Here we exclude the single 13.5 ka age from Group B moraines in favor of the other three tightly grouped ages on the landform. Use of the 13.5 ka age would create a period of overlap during which both moraine Groups A and B could have been deposited. Because moraine B is 2 km upvalley from moraine Group A they were not deposited at the same time, and Group B is younger than Group A. It is the combination of three tightly grouped absolute ages in conjunction with the relative chronology established by the geomorphology that leads us to reject the 13.5 ka age. Ice retreated from Group A1 end moraines, and they stabilized between 15.5 ka and 13.0 ka. Ages from Group A2 lateral moraines appear to straddle the ages of Groups A1 and B. Thus, our current interpretation is that they were deposited during a time when ice extended beyond the bedrock step, but they were not vacated and fully stabilized until ice retreated from moraine Group B.

Discussion and paleoclimatic implications

Comparison of the Illimani moraine ages to existing ice-core records is complicated by the fact that the range of ages associated with the moraines overlaps periods of abrupt climate change indicated in the ice-core records (Fig. 6). Most notably, the probability plot for Group A1 moraines begins during a dry period, peaks during a wet period, and finally the tail ends during a dry period as determined by the lake-level data of Baker et al. (2001a). The probability plot for moraine Group B similarly falls on a boundary between wet and dry conditions that may be responsible for the retreat of the glacier from the moraine. Although the early Holocene was previously believed to

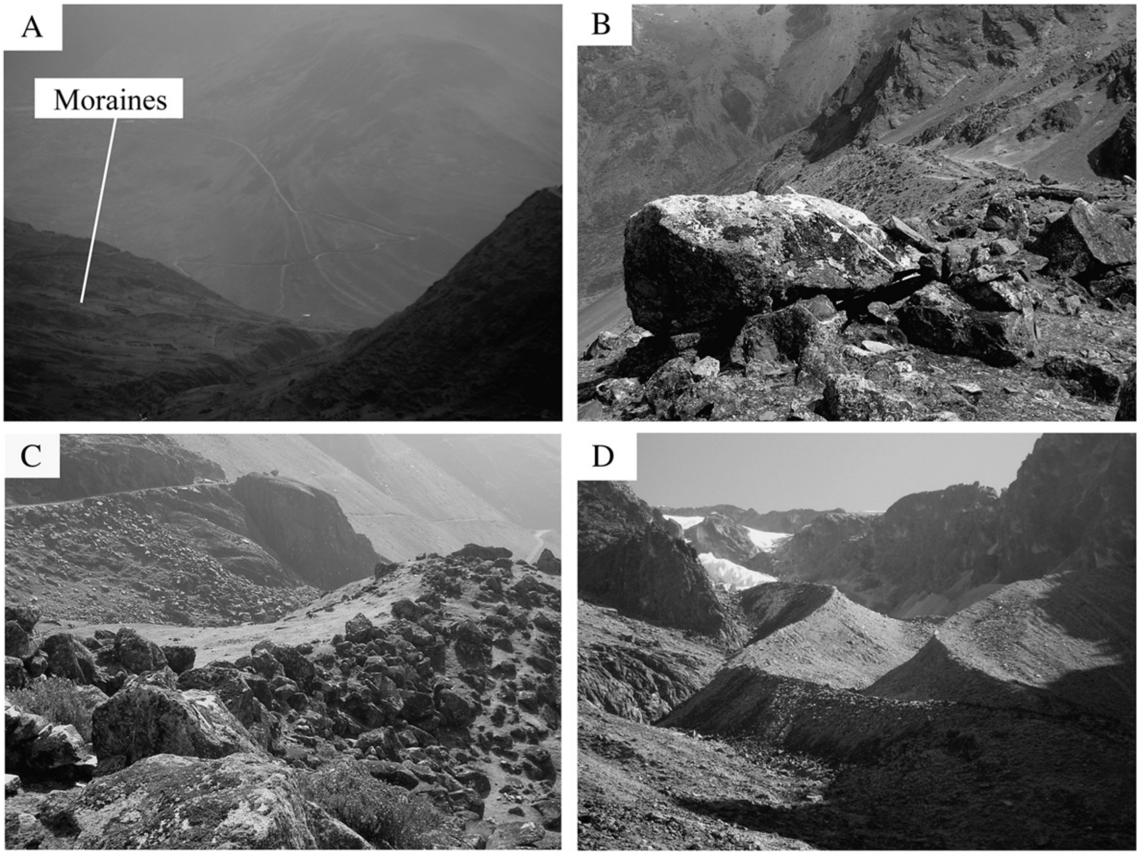

Figure 3. Views of the moraine sets described in this study. A. View from atop the bedrock step looking downvalley towards the Group A1 end moraines. B. View upvalley at the left lateral Group A2 moraine. C. The rocky deposit in the foreground extending to the right side of the photograph is the end moraine of Group B. Note the steep drop in the valley profile just downvalley from this moraine. D. Looking up the tributary valley at the laterals and end moraines of Group C.

be a time of restricted glacier extent (Seltzer, 1990), new data from the tropical Andes (Licciardi et al., 2009) suggest the presence of early Holocene glacier advances concomitant with Northern Hemisphere glacier advances. Licciardi et al. (2009) suggest that the broad correlation in the ages of Holocene glacial deposits indicates climate linkages between the North Atlantic region and the tropics. The Group C moraine dates to a period that corresponds with other dated moraines in the Eastern Cordillera (Rodbell, 1990) and perhaps the Western Cordillera (Smith et al., 2009).

Three ice-core records from tropical Andean ice cores extend beyond the Holocene. These include the ice cores collected from Nevado Sajama (Thompson et al., 1998) in the Western Cordillera and Nevado Illimani (Ramirez et al., 2003) in the Eastern Cordillera of Bolivia as well as Nevado Huascaran in the Cordillera Blanca, Peru (Thompson et al., 1995). The isotopic records from Illimani and Huascaran are largely the same (Ramirez et al., 2003). Initially, oxygen isotopic records from the tropics were interpreted to indicate changes in temperature (Thompson et al., 1995, 1998) based on the remarkable similarity to oxygen isotopic records from high latitudes. More recent work comparing meteorological records to isotopic records has shown a much stronger correlation between changes in precipitation and changes in oxygen isotopic values (Hardy et al., 2003; Hoffmann et al., 2003; Vuille et al., 2003). Although research continues to be conducted on this relationship, it appears that isotopic fluctuations track changes in precipitation more closely than changes in temperature in the tropical Andes as was originally suggested by Dansgaard (1964). Nonetheless, comparison of present estimates of moraine ages to published isotopic records of nearby glacial ice shows a more complex relationship.

The notable climatic inference derived from the present study comes from the comparison of former ELAs across the Altiplano. Regardless of the relative importance of temperature and precipitation on glacier mass balance, the ELA gradient at a given time is primarily controlled by precipitation (Lie et al., 2003). The modern ELA in the central Andes rises to the south and to the west (Seltzer, 1990; Klein et al., 1999) as a result of decreasing precipitation in these directions. Estimates of the modern ELA in the Cordillera Vilcanota and Quelccaya Ice Cap region of southeastern Peru range between 5100 m and 5300 masl (Mercer and Palacios, 1977; Thompson, 1979; Mark et al., 2002). Mass-balance measurements at Zongo Glacier in the Cordillera Real on the eastern margin of the Altiplano put the mean ELA at 5270 masl in northeastern Bolivia (Francou et al., 1995;

Table 4
Former ELAs relative to the modern ELA of 5270 masl.

Moraine group	Elevation of end moraines (m)	Extent of lateral moraines (m)	AAR 77% paleo-ELA (m)	AAR 66% paleo-ELA (m)	THAR method paleo-ELA (m)	THAR method change in ELA (m)	THAR method temperature change (°C)
A	4000	4677	4640	4865	4870	400	−3.0
B	4378	–	4840	5040	5110	160	−1.2
C	4600	5187	5055	5230	5250	20	−0.2

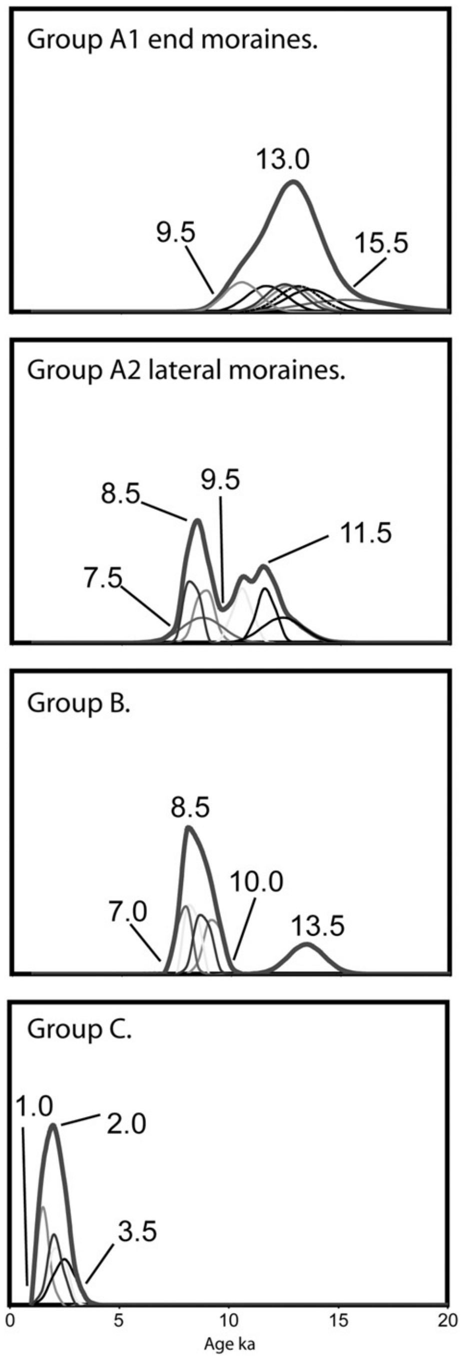

Figure 4. Probability plots showing the age distributions of moraine Groups A1, A2, B and C. Numbers refer to ages at the peaks of the distributions as well as the highs and lows surrounding the peaks.

Wagnon, et al., 1999). At Nevado Sajama in the Western Cordillera of northern Bolivia, the modern ELA is 5630 masl based on more than a decade of remotely sensed images (Arnaud et al., 2001). South of Sajama (18°S) the ELA rises above the 6000 m peaks. These data indicate that the modern ELA is a strong reflection of the precipitation gradient. In the central Andes, precipitation is derived largely from the Atlantic. Thus, the Eastern Cordillera receives more precipitation and has lower ELAs than the Western Cordillera. The lack of glaciers between 18°S and 27°S results from neither tropical (i.e., easterly) nor mid-latitude (i.e., westerly) precipitation penetrating to these latitudes in sufficient quantities to maintain glaciers (Ammann et al., 2001). Although the regional slope of the ELA rises to the west and south, the slope has changed over time.

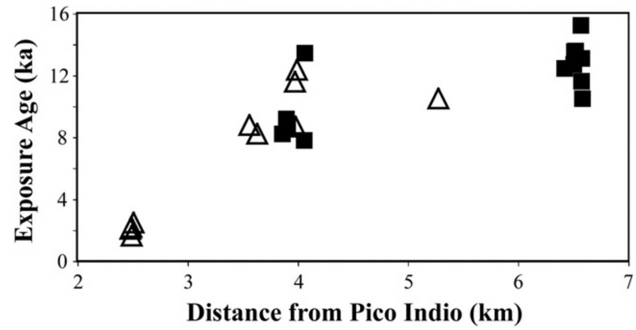

Figure 5. Age distance plot showing calculated ages and distance downvalley from Pico Indio. Solid squares are samples collected from end moraines, and hollow triangles are samples collected from lateral moraines.

Based on the ELA data presented in this paper and other studies, it appears that the regional ELA gradient during the late glacial was much flatter than present from east to west, and it rose from south to north on the southern Altiplano (Fig. 7). This is true even if the minimum ELA, derived from the maximum elevation of the lateral moraine, is used to reconstruct the late glacial regional ELA. If the calculated late glacial ΔELA values are subtracted from what authors used as the modern ELA, then the absolute elevation of the late glacial ELA can be determined. Thus, the late glacial ELA was 4935 masl in the Cordillera Vilcanota (Mark et al., 2002), 5045 m at the Quelccaya Ice-Cap (Mark et al., 2002), 4640–4840 masl in the Cordillera Real (Seltzer, 1992, 1994), 4680–4870 masl in Pasto Grande Valley, Cordillera Real (this study), 4690 masl at Nevado Sajama (Smith et al., 2009), and 4424 masl at Cerro Azanaques on the south central Altiplano (Clayton and Clapperton, 1997).

The difference between the modern ELAs in the Cordillera Real and at Nevado Sajama is 360 m (Francou et al., 1995; Wagnon, et al., 1999; Arnaud et al., 2001), but during the late glacial the difference was between ~0 and 180 m (Seltzer, 1992, 1994; Smith et al., 2009). Since precipitation controls the slope of the modern regional ELA, it is likely that precipitation also strongly influenced the slope of the late glacial ELA. Thus, the flattening of the east to west ELA gradient suggests a change in relative amounts of precipitation with the Western Cordillera becoming nearly as wet as the Eastern Cordillera.

We suggest that the change in slope of the regional ELA was a result of increased winter precipitation from the west as suggested by Hastenrath (1971) and described by Vuille and Ammann (1997). Although often overlooked, Vuille and Ammann (1997) indicate that

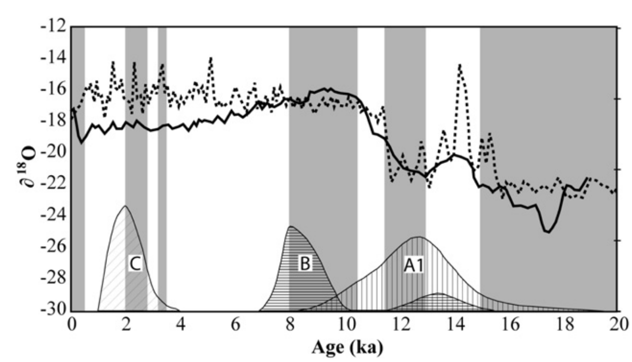

Figure 6. Plot of multiple climate proxies from the Central Andes. The dashed line is the $\delta^{18}O$ record from the Sajama ice core (Thompson et al., 1998). The solid line is the $\delta^{18}O$ record from the Huascaran ice core (Thompson et al., 1995). The gray shaded regions represent periods during which Lake Titicaca was either rising or overflowing (Baker et al., 2001a). The probability plots at the bottom give the age ranges for the end moraines Groups A1, B, and C.

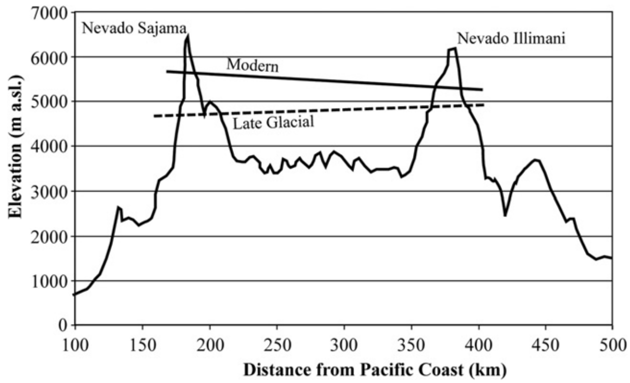

Figure 7. A schematic cross section of the Western Cordillera, Altiplano, and Eastern Cordillera shows the present ELA (solid line) and the interpreted late glacial ELA (dashed line). Note how the modern ELA rises from east to west due to decreasing precipitation in this direction. During the late glacial the ELA is nearly level across the Altiplano.

austral winter snowfall in the Western Cordillera is a regular occurrence between 18°S and 28°S. An intensification of these "cut-off" storms in the past may explain the greater late glacial ΔELA in the Western Cordillera relative to the Eastern Cordillera and the change in slope of the regional ELA gradient across the Andes.

Hastenrath (1971), working on undated moraines, reported an increase in the depression of the "Pleistocene snow-line" towards the west and south. These are the same trends that we report but with added chronological control suggesting a late glacial age. In order to explain the change in the slope of the regional ELA, Hastenrath (1971) suggested an equator-ward shift of western circulation.

Given current knowledge regarding the timing of glaciation in the tropical Andes, we suggest a western source of moisture during the late glacial as a hypothesis and not as a conclusion. Competing hypotheses to explain the apparent flattening of the regional slope of the late glacial ELA include 1) colder temperatures in the Western Cordillera than in the Eastern Cordillera, 2) increased summer precipitation from the Atlantic, 3) increased precipitation derived from paleo-lakes on the Altiplano, and 4) the various deposits used to determine late glacial ELAs are not the same age. Each of these hypotheses fails to explain fully the observed change in the slope of the regional ELA.

First, it is unlikely that tropical temperatures at the same elevation only 200 km apart differed significantly during the late glacial due to the weak coriolis effect and lack of north–south movement of air mass in the tropics (Pierrehumbert, 1995). Second, although increased late glacial precipitation derived from the east would lower ELAs in both cordilleras, and perhaps even lower Western Cordillera ELAs more than Eastern ones, it would not cause a near-leveling of the regional ELA because advected moisture would have been subjected to the same orographic constraints that it is now. While it is true that Western Cordillera glaciers are more sensitive to changes in precipitation than those in the East, it seems logical to assume that two mountain ranges with the same temperature and essentially the same ELA must be receiving similar amounts of precipitation which cannot be explained solely by an eastern source.

Third, there is evidence to suggest that large paleo-lakes on the southern Altiplano during the late glacial (Placzek et al., 2006) contributed moisture towards glacial advances. On the currently unglaciated 5140 masl Cerro Azanaques (19°S), Clayton and Clapperton (1997) suggest a mean late glacial ELA of 4424 masl. Although it is impossible to calculate modern ELAs at this latitude due to the lack of glaciers (Ammann et al., 2001), it is likely that the ELA is higher than that of Sajama, 5630 masl (Arnaud et al., 2001). However, during the late glacial this relationship was apparently reversed with lower ELAs being reported farther south at both Cerros Azanaques and Tunupa (Clayton and Clapperton, 1997; Smith et al., 2009). Blard et al. (2009) found similarly low ELAs (4380 masl) associated with late glacial moraines on Cerro Tunupa. Both of these studies suggested that increased precipitation derived from paleo-lake Tauca was responsible for the glacial advances. Whether recycled moisture from paleo-lakes reached as far north as Nevado Sajama remains an open question and awaits a more refined chronology.

It is the fourth competing hypothesis, that the glacial deposits used to reconstruct ELAs are of differing ages, that causes the most difficulties. Although the current late glacial chronologies throughout the tropical Andes overlap to a large degree, it is not possible to determine for certain that all deposits are of the same age. Regardless, if the present chronologies are accepted, then there was a pronounced change in the slope of the regional ELA that may be explained by increased winter precipitation from the west.

Besides glacial ELAs, other data support changing moisture sources during the late glacial. The work of Maldonado et al. (2005) on the pollen assemblages of rodent middens in the Atacama Desert also indicates changes in both amounts and sources of precipitation during the late glacial, with increased precipitation from the west between 24 ka and 17 ka, followed by increased precipitation from both the east and the west between 17 ka and 14 ka, followed by precipitation from the east between 14 ka and 11 ka. Thus, much of the period of proposed synchronous moraine formation (13–15 ka) in the Eastern and Western Cordilleras involved increased moisture from a westerly source.

The mass balance of north Chilean glaciers modeled by Kull and Grosjean (2000) precludes significant winter precipitation during the late glacial if winter is defined narrowly as June–September. The modeling results do not, however, exclude precipitation from the west if the period is expanded to encompass the fall, winter, and spring (May–October). The periods between summer and winter modes of circulation often include "cut-off" storms described by Vuille and Ammann (1997) that transport Pacific moisture to the Western Cordillera. If these cut-off storms are considered, then the modeling results of Kull and Grosjean (2000) are consistent with up to 30% (at 18°S) to 50% (at 22°S) of Western Cordilleran precipitation originating from the Pacific. If true, this would represent an appreciable change from modern precipitation patterns. Currently at 18°S in the Western Cordillera, only about 15% of annual precipitation is derived from the Pacific.

Not only is there evidence of increased moisture in the low latitudes of the Southern Hemisphere during the late glacial, but also there is evidence of increased aridity in the mid-latitudes of the Southern Hemisphere at the same time. Working farther south between 40° and 42°S latitude, Heusser (1981) found palynological evidence of colder and dryer conditions during between 31 and 14 ^{14}C ka BP. To explain these climatic conditions, Heusser (1981) suggests a northerly displacement of the moisture-laden westerly wind belt.

The above interpretation deviates from the more common interpretation that late glacial advances were caused by an intensification of tropical circulation for which there is much evidence (Kull, 2008; Zech et al., 2008). However, a near-flattening of the regional ELA in the central Andes is difficult to explain with only an eastern moisture source. The hypothesis of a western precipitation source is based on the idea that late glacial moraines from southern Peru and north and central Bolivia all formed at the same time. Although the absolute chronology is ambiguous, it is not inconsistent with a synchronous late glacial advance/still-stand. Thus, the interpretation of an altered slope to the regional ELA gradient forced by a change in precipitation source during the late glacial is put forth as a tentative hypothesis. There is need to improve the absolute chronologies of moraines in the tropical Andes, but the ELA gradient between the Eastern and Western Cordilleras helps clarify paleoclimatic understanding of the region.

Summary and conclusions

^{10}Be cosmogenic nuclide surface dating was used to estimate ages of glacial advances during the late glacial, early Holocene, and the last few thousand years. Results indicate that glaciers retreated from moraines at 15.5–13.0 ka, 10.0–8.5 ka, and 3.5–2.0 ka in Pasto Grande Valley on the north slope of Nevado Illimani. If the glacial advance during the late glacial at Nevado Illimani was synchronous with other glacial advances in both the Eastern and Western Cordilleras, then a marked flattening in gradient of the regional ELA occurred during the late glacial. In turn, a flat east–west ELA gradient supports the idea of increased importance of precipitation from the west during the late glacial period.

Acknowledgments

Thanks to J.M. Escobar and M. Escobar for logistics in Bolivia. Thanks to J. Dortch for instruction and assistance in the laboratory. The fieldwork was funded in part by GSA Grant Number 8405-06. Thanks also to M. Kaplan, R. Zech, and two anonymous reviewers for helpful comments on prior drafts of this manuscript.

References

Ammann, C., Jenny, B., Kammer, K., Messerli, B., 2001. Late Quaternary glacier response to humidity changes in the arid Andes of Chile (18–29° S). Palaeogeography, Palaeoclimatology, Palaeoecology 172, 313–326.
Arnaud, Y., Muller, F., Vuille, M., Ribstein, P., 2001. El Niño-Southern Oscillation (ENSO) influence on a Sajama volcano glacier (Bolivia) from 1963 to 1998 as seen from Landsat data and aerial photography. Journal of Geophysical Research 106 (No. D16), 17,773–17,784.
Baker, P.A., Seltzer, G.O., Fritz, S.C., Dunbar, R.B., Grove, M.J., Tapia, P.M., Cross, S.L., Rowe, H.D., Broda, J.P., 2001a. The history of South American tropical precipitation for the past 25,000 yrs. Science 291, 640–643.
Baker, P.A., Rigsby, C.A., Seltzer, G.O., Fritz, S.C., Lowenstein, T.K., Niklas, B.P., Veliz, C., 2001b. Tropical climate changes at millenial and orbital timescales on the Bolivian Altiplano. Nature 409, 698–701.
Balco, G., Stone, J.O., Lifton, N.A., Dunai, T.J., 2008. A complete and easily accessible means of calculating surface exposure ages or erosion rates from ^{10}Be and ^{26}Al measurements. Quaternary Geochronology 8, 174–195.
Benn, D.I., Owen, L.A., Osmaston, H.A., Seltzer, G.O., Porter, S.C., Mark, B., 2005. Reconstruction of equilibrium-line altitudes for tropical and sub-tropical glaciers. Quaternary International 138–139, 8–21.
Blard, P.H., Lavé, J., Farley, K.A., Fornari, M., Jiménez, N., Ramirez, V., 2009. Late local glacial maximum in the Central Altiplano triggered by cold and locally-wet conditions during the paleolake Tauca episode (17–15 ka, Heinrich 1). Quaternary Science Reviews 28, 3414–3427.
Briner, J.P., Kaufman, D.S., Manley, W.F., Finkel, R.C., Caffee, M.W., 2005. Cosmogenic exposure dating of late Pleistocene moraine stabilization in Alaska. Geological Society of America Bulletin 117, 1108–1120.
Clayton, J.D., Clapperton, C.M., 1997. Broad synchrony of a Late-glacial glacier advance and the highstand of palaeolake Tauca in the Bolivian Altiplano. Journal of Quaternary Science 12, 169–182.
Dansgaard, W., 1964. Stable isotopes in precipitation. Tellus 16, 436–468.
Desilets, D., Zreda, M., 2003. Spatial and temporal distribution of secondary cosmic-ray nucleon intensities and applications to in situ cosmogenic dating. Earth and Planetary Science Letters 206, 21–42.
Desilets, D., Zreda, M., Prabu, T., 2006. Extended scaling factors for in situ cosmogenic nuclides: new measurements at low latitude. Earth and Planetary Science Letters 246, 265–276.
Dunai, T.J., 2001. Influence of secular variation of the geomagnetic field on production rates of in situ produced cosmogenic nuclides. Earth and Planetary Science Letters 193, 197–212.
Francou, B., Ribstein, P., Saravia, R., Tiriau, E., 1995. Monthly balance and water discharge of an inter-tropical glacier: Zongo Glacier, Cordillera Real, Bolivia, 16°S. Journal of Glaciology 42, 61–67.
German Alpine Club, 1990. Alpenvereinskarte. Cordillera Real Süd, Illimani.
Gosse, J.C., Phillips, F.M., 2001. Terrestrial in situ cosmogenic nuclides: theory and application. Quaternary Science Reviews 20, 1475–1560.
Hardy, D.R., Vuille, M., Bradley, R.S., 2003. Variability of snow accumulation and isotopic composition on Nevado Sajama, Bolivia. Journal of Geophysical Research 108 (NO. D22), 4693, doi:10.1029/2003JD003623, 2003.
Harrison, S.D., 2005. Snowlines at the last glacial maximum and tropical cooling. Quaternary International 138–138, 5–7.
Hastenrath, S.L., 1971. On the Pleistocene snow-line depression in the arid regions of the South American Andes. Journal of Glaciology 59, 255–267.
Haug, G.H., Hughen, K.A., Sigman, D.M., Peterson, L.C., Röhl, U., 2001. Southward migration of the intertropical convergence zone through the Holocene. Science 293, 1304–1308.
Heusser, C.J., 1981. Palynology of the last interglacial-glacial cycle in midlatitudes of southern Chile. Quaternary Research 16, 293–321.
Hoffmann, G., Ramirez, E., Taupin, J.D., Francou, B., Ribstein, P., Delmas, R., Durr, H., Gallaire, R., Simoes, J., Schotterer, U., Stievenard, M., Werner, M., 2003. Coherent isotope history of Andean ice cores over the last century. Geophysical Research Letters 30 (No. 4), 1179.
Jordan, E., 1999. Glaciers of Bolivia. In: Williams, R.S., Ferrigno, J.G. (Eds.), Satellite Image Atlas of Glaciers of the World: South America. United States Geological Survey Professional Paper 1386-I, United States Government Printing Office, Washington D.C.
Kaser, G., Osmaston, H., 2002. Tropical Glaciers. Cambridge University Press, Cambridge. 207 pp.
Klein, A.G., Seltzer, G.O., Isacks, B.L., 1999. Modern and last local glacial maximum snowlines in the Central Andes of Peru, Bolivia, and Northern Chile. Quaternary Science Reviews 18, 63–84.
Kull, C., 2008. Late Pleistocene glaciation in the Central Andes: temperature versus humidity control — a case study from the eastern Bolvian Andes (17°S) and regional synthesis. Global and Planetary Change 60, 148–164.
Kull, C., Grosjean, M., 2000. Late Pleistocene climate conditions in the north Chilean Andes drawn from a climate-glacier model. Journal of Glaciology 46, 622–632.
Lal, D., 1991. Cosmic ray labeling of erosion surfaces: in situ nuclide production rates and erosion models. Earth and Planetary Science Letters 104, 424–439.
Licciardi, J.M., Schaefer, J.M., Taggart, J.R., Lund, C.D., 2009. Holocene glacier fluctuations in the Peruvian Andes indicate northern climate linkages. Science 325, 1677–1679.
Lie, Ø., Dahl, S.O., Nesje, A., 2003. A theoretical approach to glacier equilibrium-line altitudes using meterological data and glacier mass-balance records from southern Norway. Holocene 13, 365–372.
Lifton, N.A., Bieber, J.W., Clem, J.M., Evenson, P., Humble, J.E., Pyle, R., 2005. Addressing solar modulation and long-term uncertainties in scaling secondary cosmic rays for in situ cosmogenic nuclide applications. Earth and Planetary Science Letters 239, 140–161.
Maldonado, A., Betancourt, J.L., Latorre, C., Villagran, C., 2005. Pollen analyses from a 50,000-yr rodent midden series in the southern Atacama Desert (25° 30′ S). Journal of Quaternary Science 20, 493–507.
Mark, B.G., Seltzer, G.O., Rodbell, D.T., Goodman, A.Y., 2002. Rates of deglaciation during the last glaciation and Holocene in the Cordillera Vilcanota–Quelccaya Ice Cap region, southeastern Peru. Quaternary Research 57, 287–298.
Meierding, T., 1982. Late Pleistocene glacial equilibrium-line altitudes in the Colorado Front Range: a comparison of methods. Quaternary Research 18, 289–310.
Mercer, J.H., Palacios, O.M., 1977. Radiocarbon dating of the last glaciation in Peru. Geology 5, 600–604.
Phillips, F.M., Zreda, M.G., Gosse, J.C., Klein, J., Evenson, E.B., Hall, R.D., Chadwick, O.A., Sharma, P., 1997. Cosmogenic ^{36}Cl and ^{10}Be ages of Quaternary glacial and fluvial deposits of the Wind River Range, Wyoming. Geological Society of America Bulletin 109, 1453–1463.
Pierrehumbert, R.T., 1995. Thermostats, radiator fins, and the local runaway greenhouse. Journal of Atmospheric Science 52, 1784–1806.
Placzek, C., Quade, J., Patchet, P.J., 2006. Geochronology and stratigraphy of late Pleistocene lake cycles on the southern Bolivian Altiplano: implications for causes of tropical climate change. Geological Society of America Bulletin 118, 515–532.
Porter, S.C., 2001. Snowline depression in the tropics during the last glaciation. Quaternary Science Reviews 20, 1067–1091.
Ramirez, E., Hoffmann, G., Taupin, J.D., Francou, B., Ribstein, P., Caillon, N., Ferron, F.A., Landais, A., Petit, J.R., Pouyaud, B., Schotterer, U., Simoes, J.C., Stievenard, P., 2003. A new Andean deep ice core from Nevado Illimani (6350), Bolivia. Earth and Planetary Science Letters 212, 337–350.
Rodbell, D.T., 1990. Lichenometric and radiocarbon dating of Holocene glaciation, Cordillera Blanca, Peru. Holocene 2, 19–29.
Rowe, H.D., Guilderson, T.P., Dunbar, R.B., Southon, J.R., Seltzer, G.O., Mucciarone, D.A., Fritz, S.C., Baker, P.A., 2003. Lake Quaternary lake-level changes constrained by radiocarbon and stable isotope studies on sediment cores from Lake Titicaca, South America. Global and Planetary Change 38, 273–290.
Seltzer, G.O., 1990. Recent glacial history and paleoclimate of the Peruvian–Bolivian Andes. Quaternary Science Reviews 9, 137–152.
Seltzer, G.O., 1992. Late Quaternary glaciation of the Cordillera Real, Bolivia. Journal of Quaternary Science 7, 87–98.
Seltzer, G.O., 1994. A lacustrine record of late Pleistocene climatic change in the subtropical Andes. Boreas 23, 105–111.
SENAHAMI website: http://www.senamhi.gov.bo/.
Smith, J.A., Seltzer, G.O., Farber, D.L., Rodbell, D.T., Finkel, R.C., 2005. Early local last glacial maximum in the Tropical Andes. Science 308, 678–681.
Smith, C.A., Lowell, T.V., Caffee, M.W., 2009. Late glacial and Holocene cosmogenic surface exposure age glacial chronology and geomorphological evidence for the presence of cold-based glaciers at Nevado Sajama, Bolivia. Journal of Quaternary Science 24, 360–372.
Stone, J.O., 2000. Air pressure and cosmogenic isotope production. Journal of Geophysical Research 105/B10, 23,753–23,759.
Thompson, L.G., 1979. Glaciology of the Peruvian Quelccay ice cap. Boletin de la Sociedad Geologica del Peru 63, 149–158.
Thompson, L.G., Mosley-Thompson, E., Davis, M.E., Lin, P.N., Henderson, K.A., Cole-Dai, J., Bolzan, J.F., Liu, K.B., 1995. Late Glacial Stage and Holocene tropical ice core records from Huascaran, Peru. Science 269, 46–50.
Thompson, L.G., Davis, M.E., Mosley-Thompson, E., Sowers, T.A., Henderson, K.A., Zagorodnov, V.S., Lin, P.N., Mikhalenko, V.N., Campen, R.K., Bolzan, J.F., Cole-Dai, J., Francou, B., 1998. A 25,000-year tropical climate history from Bolivian ice cores. Science 282, 1858–1864.

Vuille, M., Ammann, C., 1997. Regional snowfall patterns in the high, arid Andes. Climatic Change 36, 413–423.

Vuille, M., Bradley, R.S., Werner, M., Healy, R., Keimig, F., 2003. Modeling $\partial^{18}O$ in precipitation over the tropical Americas: 1. Interannual variability and climatic controls. Journal of Geophysical Research 108 (No. D6), 4174.

Wagnon, P., Ribstein, P., Kaser, G., Berton, P., 1999. Energy balance and runoff seasonality of a Bolivian glacier. Global and Planetary Change 22, 49–58.

Zech, R., May, J.H., Kull, C., Ilgner, J., Kubik, P.W., Veit, H., 2008. Timing of late Quaternary glaciation in the Andes form 15 to 40 °S. Journal of Quaternary Science 23, 635–647.

Zhou, J., Lau, K.M., 1998. Does a monsoon climate exist over South America? Journal of Climate 11, 1020–1040.

Zreda, M.G., Phillips, F.M., Elmore, D., 1994. Cosmogenic ^{36}Cl accumulation in unstable landforms 2. Simulations and measurements on eroding moraines. Water Resources Research 30, 3127–3136.